Asian Journal of Green Chemistry 8 (2024) 81-107

Asian Journal of Green Chemistry

Review Article

View Article Online | View Journal

A Comprehensive Review on Adsorption of Dyes from Aqueous Solution by Mxenes

Farhad Ali[a], Shafaq Zahid[a], Shakir Khan[b], Shafi Ur Rehman[c], Fawad Ahmad[a,*]

[a]*Department of Chemistry, University of Wah, Quaid Avenue, Wah Cantt., Taxila, Rawalpindi, Punjab, Pakistan*
[b]*Ibn-e- Sina Institute of Technology H11/4 Islamabad 44000, Pakistan*
[c]*School of Chemical and Materials Engineering (SCME), National University of Sciences and Technology (NUST), Islamabad 44000, Pakistan*

ARTICLE INFORMATION

Submitted: 18 August 2023
Revised: 20 September 2023
Accepted: 26 September 2023
Available online: 9 October 2023

Manuscript ID: AJGC-2305-1396
Checked for Plagiarism: Yes
Language Editor:
Dr. Fatimah Ramezani
Editor who approved publication:
Dr. James Bashkin

DOI: 10.48309/ajgc.2023.412227.1435

KEYWORDS

MXene
Dye adsorption
Water Pollution
Wastewater treatment

ABSTRACT

Dyes are extensively used across a variety of industries, raising concerns about their potential to contaminate water sources. Therefore, effective and environment-friendly removal techniques are essential. The potential of MXenes as adsorbents for dye adsorption from water is thoroughly examined in this review. Two-dimensional transition metal carbides or nitrides, known as MXenes, have extraordinary physicochemical characteristics, such as a large surface area, variable surface chemistry, and superior adsorption capability. This study examined the structural properties of MXenes, their methods of production, and their special adsorption processes for dye removal. In addition, a thorough analysis of the effects of several variables, including the pH, contact time, initial dye concentration, and temperature, on the adsorption efficiency of MXenes was performed. This article also highlights the current developments in the MXenes modification to increase the effectiveness of their dye adsorption. Furthermore, this report addresses the difficulties in applying MXenes as adsorbents in practice and suggests future research avenues to overcome these restrictions. Overall, this study offers insights into the prospective use of MXenes in water treatment technologies and portrays them as promising and long-lasting adsorbents for the removal of synthetic dyes from water.

Corresponding authors, email: fawad.ahmad@uow.edu.pk (F. Ahmad).
Tel.: 923009039212.

Graphical Abstract

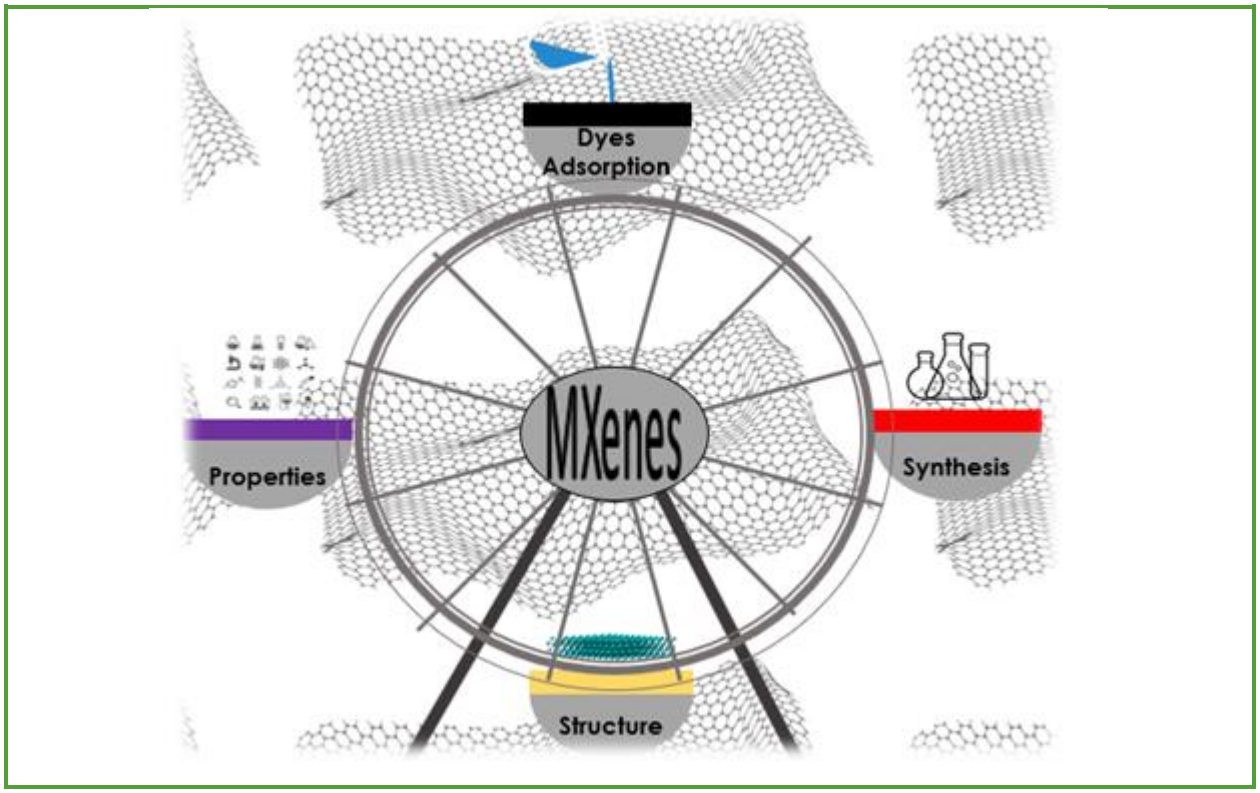

Introduction

All life on the Earth relies on water as an essential resource. It is necessary for various things, including drinking, agriculture, industry, and sanitation, and also covers approximately 71% of the earth's surface [1]. However, because of human activity and natural forces, water pollution has become a serious issue [2]. In developing nations, it is projected that 1.1 billion people lack access to safe drinking water [3] (WHO/UNICEF, Report, Global water supply, 2000). The Chicago River was significantly contaminated more than a century ago as a result of home and industrial wastewater discharge, earning it the name "Bubbly Creek" due to the apparent gas bubbles from decomposing trash. To avoid contaminating the city's drinking water source, engineers and city planners launched a significant ground-breaking initiative to redirect the river's flow away from Lake Michigan. Cutting-edge wastewater treatment techniques were also used. Today, the Chicago River is a unique example of a once-polluted watercourse transformed into a thriving and beautiful metropolitan area [4, 5].

The challenging environmental problem of water contamination has been worsened by several industries and activities. For instance, agriculture contaminates water by allowing pesticides, herbicides, and fertilizers to wash into neighboring waterways, causing chemical contamination and nutrient pollution, which promotes toxic algal blooms. Chemical pollution is frequently caused by industrial production processes discharging chemicals and heavy metals into water bodies, whereas thermal pollution is sometimes caused by the release of heated water into rivers and lakes. Mining

activities discharge dirt and sediment into streams, polluting water with sediment that can suffocate aquatic habitats. Abandoned mines may also produce acidic runoff contaminated with heavy metals. If municipal wastewater is not properly treated, contaminants and pathogens can enter the water, compromising public health and water quality. In addition, by introducing pollutants into aquatic bodies, stormwater runoff from metropolitan areas can contribute to water contamination [6-14].

Dyes are one of the most important toxins contributing to the contamination of water resources. Dyes are colorful compounds used in the dyeing process to add color to a variety of materials, including textiles, paper, and plastics. The chemical makeup of colors employed in these businesses frequently contains compounds that can harm aquatic environments as well as human health. Synthetic dyes contain complicated substances such as organic contaminants, heavy metals, and aromatic chemicals. These dangerous compounds are released into the environment when dye wastewater that has not been properly or adequately cleaned is dumped into water bodies [15-17].

According to the World Bank, the dyeing and finishing of textiles contribute between 17 and 20 percent of industrial water pollution, among which dyed water has been shown to contain 72 hazardous compounds, 30 of which are non-removable, creating a huge environmental concern for the textile sector [18]. Because dye wastewater discharge contains various contaminants that can be poisonous to both plants and animals, altering ecosystems and causing the demise of some species, it is a serious concern [19]. Even at low concentrations (0.001 mg/L), organic dyes cause human cancer and pose a serious threat to human health [20]. Furthermore, dyes degrade aesthetic value because they are noticeable in water bodies owing to their vivid and bright colors. Unnatural colors can alter how people perceive the quality of water, discourage recreational activities, and negatively affect tourism, all of which can have an economic impact on towns that depend on water-based industries. Therefore, a method for treating wastewater containing organic dyes is widely desired [21, 22].

Dye removal from aqueous solutions can be achieved using various techniques. Coagulation, flocculation, adsorption, membrane filtration, chemical oxidation, biological processes, and advanced oxidation are some of these techniques [23-25]. Chemicals were added during coagulation to balance the charges on the dye molecules and solid particles. The production of larger particles (flocs) is then promoted by flocculation, which aids in their precipitation and removal from water [26]. By combining these two methods, the dyes in the water were successfully removed. Soraya Ihaddaden *et al.* [27] studied a bentonite-based coagulant and a cactus-based flocculant in the elimination of a methylene blue (MB) from an aqueous solution and observed 98.99% removal of MB. Md. Nahid Pervez [28] also reported the 94% degradation of MB dye using PVA membranes.

Advanced methods for removing dyes from wastewater include ozonolysis, photocatalysis, and membrane filtering. Ozonolysis uses ozone to break down dyes into less harmful byproducts, and photocatalysis uses UV-activated substances such as titanium dioxide to break down dyes. Amane Jada *et al.* [29] explored the ZnO/Montmorillonite photocatalyst for the removal of RhB dye from water and got excellent results. Membrane filtration physically separates and excludes dye molecules. Ziran Su *et al.* [30] studied the membrane filtration method for the removal of Azo dyes in an enzymatic membrane reactor

and reported that after three consecutive enzyme membrane cycles, all dyes had almost completely lost their color. Depending on factors such as dye type, concentration, and particular requirements of the wastewater treatment process, each method can be used, and each method has specific advantages [31-36].

Being eco-friendly and cost-effective, adsorption is frequently regarded as the best method for dye removal from aqueous solutions. High removal efficiencies, which allow the successful removal of various dye molecules from water, are one of its key features. Adsorption is a flexible remedy for numerous types of dye pollution because it works for both organic and inorganic dyes. It also provides diversity in terms of adsorbent selection, enabling the selection of substances that target the required dye molecules [37-39]. The most common adsorbents used are chitosan, MOF, metal oxides, and activated alumina. Abida Mariyam *et al.* [40] investigated the adsorption of MB using tetrazole-based porous MOF and found a 90% adsorption capacity. However, these adsorbents are less efficient, expensive, and have smaller surface areas for adsorption [41].

To make the adsorption process more efficient, we used carbon-based materials, such as activated carbon and CNTs [42]. Yahiya Kadaf Manea [43] used Al-Li/Th-LDH@CNT as an adsorbent and removed 94..1% of Cr^{+6}. However, these carbon materials are not used on a large scale because of their high cost [44]. Recently, 2D nanomaterials such as TMDs, Graphene, and Black Phosphorus (BP) have been used in various industries because of their exceptional electrical, optical, mechanical, and thermal properties [45].

MXenes, created in 2011, are the newest additions to the 2D universe. Ti_3C_2 (titanium carbide) was the first MXene. Hydrofluoric acid (HF) was used to selectively etch Al atoms from Ti_3AlC_2, a layered hexagonal ternary carbide, while the process was carried out in ambient circumstances. MXenes today represent a sizable family of transition metal carbides, nitrides, and carbonitrides as a result of enormous advancements in this field [46, 47].

MXenes are used in sensors, supercapacitors, batteries, catalysts, and biomedical devices, demonstrating their extensive potential for advancing science and industry [48, 49]. MXenes have also received considerable attention as potential adsorbents for various applications, including dye removal. MXenes are effective adsorbents owing to their numerous distinctive characteristics. They have initially a large specific surface area per gram, usually between hundreds and thousands of square meters. This wide surface area offers many locations for dye molecules to bind, enabling their effective removal from contaminated water. MXenes are also extremely durable and reusable as adsorbents owing to their exceptional mechanical and chemical resilience. It is essential for efficient and long-lasting water treatment procedures that their structural integrity endure repeated adsorption-desorption cycles [50-52]. Yuan Lei [53] used Ti_3C_2–SO_3H as an adsorbent for the MB adsorption and reported an adsorption capacity of 111.11mg/g.

Our in-depth examination provides a novel viewpoint on MXenes for dye adsorption by highlighting current developments and new problems. We shall conduct a thorough investigation of MXenes as adaptable materials for dye adsorption in the following sections of this review. We will begin by explaining the synthesis processes used to create MXenes and reveal their special structural and physicochemical characteristics, which make them remarkable adsorbents. We also explore the crucial elements, characterization, and

optimization techniques involved in enhancing the MXenes capacity to adsorb different dye molecules. We seek to present a holistic view of the possibilities and difficulties in using MXenes for dye adsorption applications by thoroughly analyzing their synthesis, characteristics, optimization aspects, and future possibilities.

MXenes

MXenes were first discovered in 2011 by Drexel University scientists who investigated the synthesis of two-dimensional (2D) carbides and nitrides called MAX phases. MAX phases are layered compounds with the formula $M_{n+1}AX_n$, where M is an early transition metal, A is an A-group element (often silicon or aluminum), X is carbon or nitrogen, and n is the number of atomic layers. From these phases, MXenes are produced (Figure 1)[54, 55].

In 2011, Prof. Michel W. Barsoum *et al.* at Drexel University revealed that 2D transition metal carbides may be created by selectively etching the A-layer from the MAX phases using hydrofluoric acid. The A-layer is eliminated during this etching procedure, leaving transition metal carbide, nitride, or carbonitride sheets that make up the MXene structure. The X layer (carbon/nitrogen) was placed on top of the transition metal layer that served as the core layer. By combining the letters "M" from the transition metal, "X" from carbon/nitrogen, and "ene" to indicate their 2D character, these newly created materials were named MXenes [55, 56].

Owing to their layered structure and large surface area, the resulting MXenes are well suited for various applications such as energy storage, catalysis, and electronics. Through surface functionalization, MXenes can be further altered by adding various functional groups to customize their characteristics for specific uses. A growing family of MXenes contains a wide range of compositions built on several transition metals, offering a rich foundation for additional studies and exploration of their potential in numerous domains [55, 57].

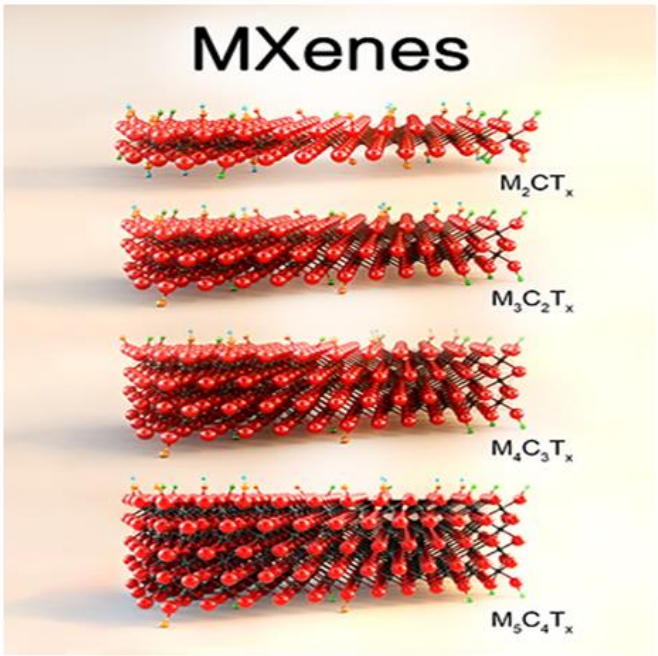

Figure 1. Structure of different MXenes (image: Prof. Armin Vahid, Mohammadi, and Yury Gogotsi, Drexel University) Copyright (2022) Elsevier

MXenes synthesis

MXenes can be prepared by various techniques. Here are several methods that are frequently used.

Selective etching method

The selective etching method is a vastly used technique for the MXenes synthesis, by carefully removing the "A" element, often aluminium, from the MAX phase precursor in several phases, a multilayer MXene structure is left behind [58]. The MAX phase, a multilayer complex composed of a transition metal, an "A" element, and carbon or nitrogen, was initially created in the process. The MAX phase is then synthesized, and exfoliation techniques are used to separate it into separate layers [59]. The MAX phase layers are next subjected to etching in an appropriate etchant solution, which is commonly a combination of hydrofluoric acid and fluoride salt as shown in the Figure 2. The "A" element from the MAX phase levels is specifically targeted and eliminated by this etchant. The delaminated MXene layers are retrieved after the sample has been properly cleaned to remove any remaining etchant. The MXenes surface can be further altered by functionalization according to the intended application. This selective etching technique allows researchers to control the MXenes synthesis, permitting the creation of multilayer MXenes with various transition metals and X elements. The interlayer spacing can be altered to provide tunable qualities for particular applications by selectively removing the "A" element [60-62]. A Study by Youbing Li [63] showed that $CuCl_2$ Lewis molten salt was submerged in Ti_3SiC_2 MAX phase at 750 °C followed by $Ti_3C_2T_x$ MXene was produced as a result of the reaction between Ti_3SiC_2 and $CuCl_2$. After additional washing with ammonium persulfate (APS) solution, MS-$Ti_3C_2T_x$ MXene was produced.

Intercalation and exfoliation methods

In this procedure, ions or other guest species were inserted between the layers of the precursor material.

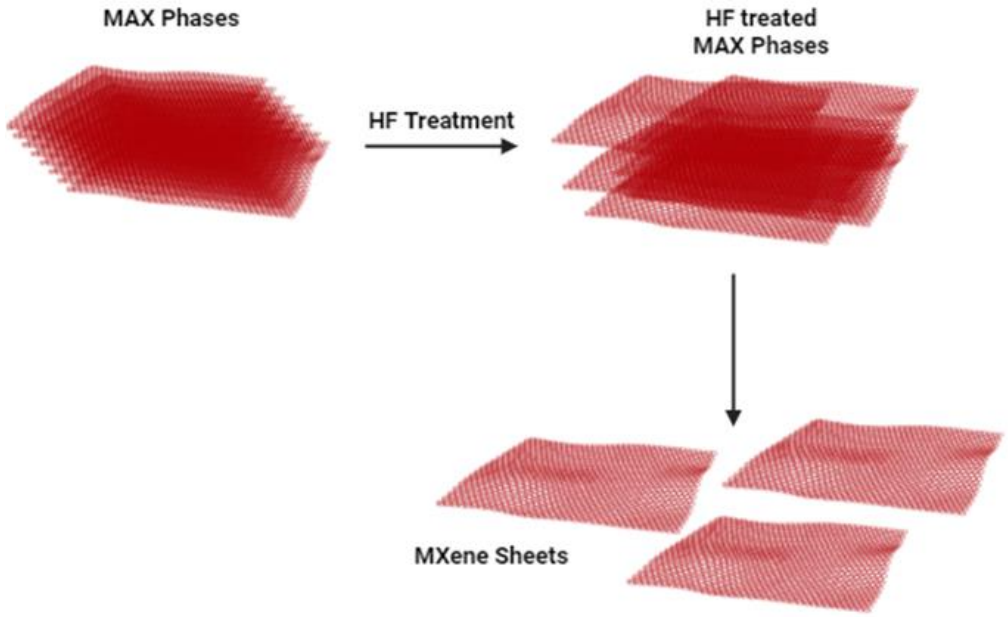

Figure 2. Selective etching method of MXenes synthesis

The selection of an appropriate precursor material, frequently a MAX-phase compound, marks the start of the procedure. During the intercalation step, the precursor material is submerged in a solution containing intercalants, which are typically ions or tiny molecules. The interlayer voids of the precursor material were invaded by the intercalants, increasing the interlayer spacing. The larger interlayer spacing facilitates the separation of individual layers during the exfoliation stage that follows the intercalated precursor. Exfoliation uses mechanical or acoustic techniques to separate MXene layers, followed by washing to remove the byproducts and intercalants. With the use of different intercalants, this technique enables the controlled synthesis of MXenes, changing their characteristics for certain applications [64-66]. Xuan *et al.* [67] presented an organic base-driven intercalation and delamination of TiC (Figure 3A). Another study by Li *et al.* [68] used KOH and water as etchants for the MXenes synthesis (Figure 3B).

Electrochemical exfoliation

In this technique, MXene layers were selectively etched and exfoliated using an electrochemical procedure. A MAX phase or precursor material submerged in an electrolyte solution is subjected to a voltage. The A-layer is selectively etched by an electric field, which then encourages exfoliation of the MXene sheets [69, 70]. To produce a layer of Ti_2CT_x MXene on Ti_2AlC, Wanmei Sun *et al.* [71] effectively demonstrated the electrochemical etching of Al from porous Ti_2AlC electrodes in dilute hydrochloric acid. To the best of our knowledge, this is the first report of etching the Al layer from the MAX phase in a fluoride-free solution. In another study, Pang *et al.* [72] investigated HF-free MXene synthesis via thermal-assisted electrochemical etching (Figure 3C).

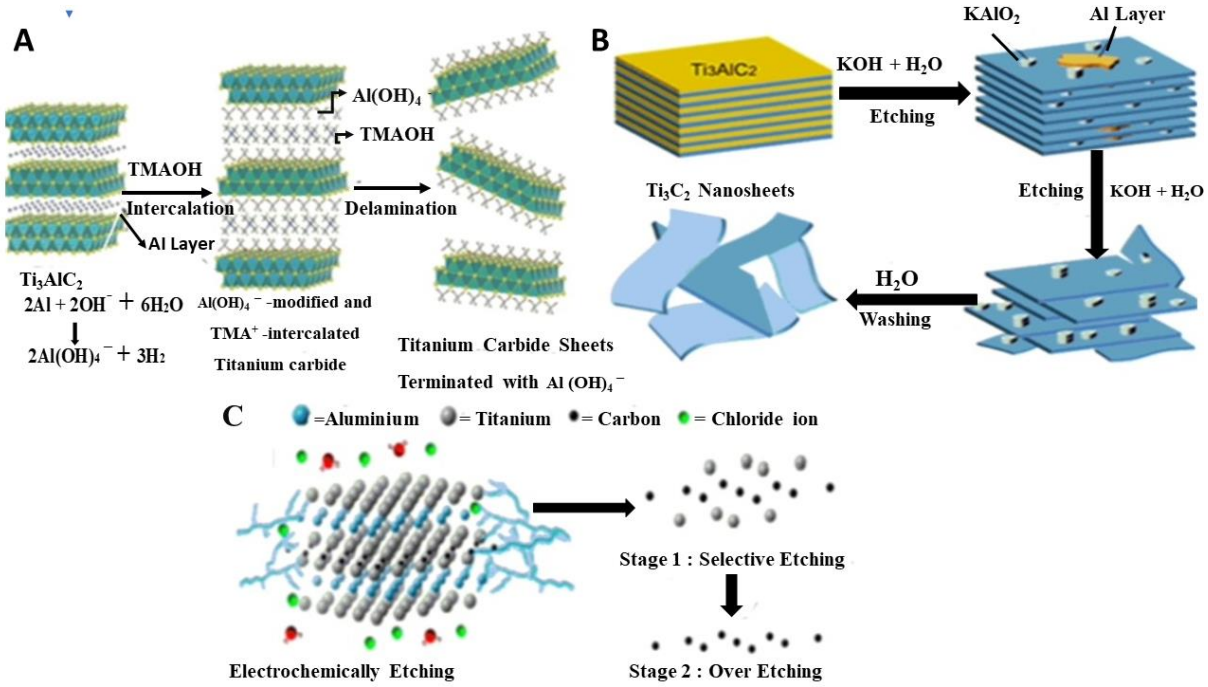

Figure 3. A) Organic-base-driven TiC [67] [Copyright (2016) Wiely], B) KOH method for Ti_3C_2 [68] [Copyright (2017) American Chemical Society], and C) electrochemical etching of Ti_2AlC in HCl [72] [Copyright (2019) American Chemical Society]

Properties of MXenes

The highest Young's modulus range, tunable bandwidth, and improved electric and thermal conductivities are acknowledged as special and advantageous characteristics of MXenes. However, along with graphene, the hydrophilic nature of MXenes combined with their improved thermal conductivities sets them apart from other 2D materials [73].

Various elements, including the individual MXene composition, synthesis process, and surface functionalization, may affect the properties of the prepared genes [74]. Here are some general traits connected to Mxenes.

Structural properties

The crystal structure of MXenes is hexagonal close-packed, like that of their MAX-phase forerunner. With X atoms filling octahedral positions, the M atoms are organized in a compact form. Like other 2D materials, MXenes' layers are joined together by Van der Waals forces [75].

Typically, acidic fluoride-containing aqueous solutions are used to create MXenes, resulting in surface terminations of OH, O, and F. The MXenes characteristics are significantly influenced by these terminations. Different terminations have an impact on the stability, mechanical characteristics, and electrical structures of MXenes, according to computational research. Charge transfers from interior bonds to the outer surface, for instance, improve the thermodynamic stabilization and strength of oxygen-functionalized MXenes. Even post-synthesis techniques can be used to achieve particular terminations; little research has been done on this subject. One such example is S-functionalized Ti_3C_2, which, as predicted by Meng *et al.* [76] exhibits metallic behavior, a stable structure, a low diffusion barrier, and great storage capacity for Na-ion batteries.

Electronic and electrical properties

By adjusting functional groups, material balance, or creating solid solutions, it is possible to vary the electric and electronic characteristics of MXenes, two crucial aspects. Pressed MXene films have electrical conductivities that are higher than carbon nanotubes and derivatives of graphene oxide and comparable to graphene multilayers. Simulated functions have higher conductivities than experimental observations because of the increase in resistivity that comes with adding layers and the obstruction caused by functional molecules [77, 78].

Due to variations in surface functionalities, defect concentration, d-spacing between MXene particles, delamination yield, and lateral dimensions brought on by etching procedures, the electrical conductivities of Ti_3C_2Tx MXenes range from 850 to 9870 S/m [79]. MXenes with fewer flaws and improved lateral expansion are produced using less fluoric acid and in short term result in higher electrical conductivity ranges. Their electrical conductivities can be also impacted by environmental wetness, making them appropriate for sensing applications. Alkaline and thermal surface modifications can enhance the electrical characteristics, leading to a two-order increase in conductivity magnitude. This increase can be attained by modifying intercalated ions and molecules as well as surface functions [80-83]. Table 1 presents different MXene nanocomposites with their electrical conductivity.

Table 1. Mxenes nanocomposites with their electrical conductivities

Material	Method of Preparation	Electrical Conductivity (S/cm)	References
TI_3C_2	Hot Press Sintering	850	[84]
Mo_2CT_x	Vacuum-assisted Filtration	1.2	[85]
$TI_3C_2T_x$	Hydrothermal	4556	[86]
90% MXene/10% rGO	Hydrothermal	1231	[87]

Table 2. Summary of MXenes modifications

Types	Process	Conduction	Mechanical Property	Stability	Hydrophilicity	References
Atomic Doping	NH_3; Solvothermal	Increases	-	-	-	[95]
Original Surface termination	Ar; heat treatment	Increases	increases	Increases	-	[96, 97]
Materials Compounding	PVA; vacuum filtration	Decreases	Increases	Increases	Decreases	[98]
External Surface termination	p-phenyl SO_3H	Decreases	Decreases	-	-	[99]

Mechanical properties

Young's modulus, which assesses a material's stiffness and resistance to elastic deformation, is one of the most important indicators of mechanical strength. The high Young's modulus values of MXenes, which frequently range from tens to hundreds of GPa, are well-recognized. For instance, Young's modulus of Ti3C2Tx MXene is about 330 GPa, while Young's moduli of other MXenes like Nb_2C and V_2C are much higher [88]. With an average tip radius of 7 nm, MXene membranes have an effective Young's modulus of 333 30 GPa and a breaking strength of 17.3 1.6 GPa. It is interesting to note that Ti_3C_2 has Young's modulus of 502 GPa as determined by molecular dynamics simulations [89, 90]. It is discovered that the film thickness has a significant impact on the tensile strength of MXene. When the thickness of the MXene film is increased from 2.3 m to 17 m, Luo *et al.* showed that the elastic modulus and tensile strength decrease from 17 GPa to 8 GPa and 61 MPa-36 MPa, respectively [91].

In addition to have a high Young's modulus, MXenes have a strong physical character. The strength of MXenes often ranges from several hundred to several thousand megapascals (MPa), which is high. As an illustration, $Ti_3C_2T_x$ MXene is mentioned to have a strength of about 400 Mpa [92]. According to research by Liang *et al.* [93], the addition of 3 wt% MXene increases ceramics' fracture toughness by 7.6 MaPam1/2, or 36% more than ceramics without any additions.

Another crucial component of mechanical behavior is flexibility. MXenes may bend and deform because of their layered structure, which gives them a certain amount of flexibility. Due to their adaptability, MXenes are attractive candidates for several applications, such as flexible electronics and wearable technology [94]. It is important to remember that the precise mechanical characteristics of MXenes can change depending on elements including composition, doping, synthesis process, and the

presence of defects or functional groups. The research that has been done to date on changing the MXenes properties is summarized in Table 2, which is separated into two categories: atomic doping and termination altering are examples of chemical modification of physical composites (compounding of materials). Table 2 provides a summary of the specific process method, conductivity changes, stability, mechanical qualities, and hydrophilicity of MXenes.

MXenes as adsorbents for dye adsorption

The process of dragging dye molecules from a liquid solution onto a solid surface and holding them there is referred to as dye adsorption. The textile industry, environmental cleanup, and wastewater treatment are just a few of the areas where this phenomenon is significant [100]. Different mechanisms help the adsorption process when a dye-containing solution comes into contact with a solid adsorbent material such as activated carbon, graphene oxide, or metal oxides [101]. While chemical adsorption includes chemical bonding between the dye molecules and the adsorbent surface, physical adsorption involves weak intermolecular interactions between the dye molecules and the adsorbent surface. While chemical adsorption creates stronger and more durable connections, physical adsorption is reversible [102-104].

Mxenes have a wide surface area and variable surface chemistry, making them ideal adsorbents for dye adsorption. Compared to the other adsorbents, their two-dimensional layered structure offers a large specific surface area, allowing for improved adsorption capacity. Adsorption performance may be optimized for effective dye capture and removal thanks to the tunable surface chemistry, which permits modification to increase affinity and selectivity towards particular dye molecules [105-107].

Characterization of adsorbent

It is essential to characterize Mxenes as adsorbents to comprehend adsorption mechanisms and evaluate their effectiveness. The interaction of dye molecules with Mxenes is studied by techniques such as surface area analysis, pore size distribution, and surface chemistry study. Design and performance are optimized using this knowledge. The maximal dye adsorption capacity of Mxenes may be calculated using variables like specific surface area and functional group density, which is crucial for assessing their viability and efficiency in real-world applications[108, 109].

SEM and TEM

When MXenes are used as adsorbents, SEM and TEM examination can reveal important details regarding the morphological and structural changes that take place during dye adsorption. SEM photos depict a layered structure with a smooth surface before adsorption, while TEM verifies that MXenes are two-dimensional materials. Adsorption success is demonstrated by changes in surface patterns in SEM images after adsorption, such as the creation of dye aggregates or clusters. Compared to the pre-adsorption state, these aggregates can change the texture and roughness of the surface [110-112].

TEM provides atomic-scale insights. Depending on the adsorption method and the interaction between MXenes and the dye, changes in the MXene lattice structure, such as expansion or contraction, may be seen. Asif Shahzad *et al.* [113] worked on the adsorption of Cu^{+2} on 2D $Ti_3C_2T_x$, study showed that before adsorption, the sheetlike structure of the $Ti_3C_2T_x$ aggregates is visible in SEM

micrographs (Figure 4A). The sheets were restacked with enhanced surface roughness following Cu^{2+} adsorption (Figure 4B). A significant increase in exposed surface area and successful delamination of MXene into one or more sheets were both validated by the large change in specific surface area. This increased exposed surface area is crucial for greatly enhancing the dye or metal adsorption capability. After Cu adsorption, $Ti_3C_2T_x$'s structural alterations were seen in TEM pictures. Initially, $Ti_3C_2T_x$ exhibited sheetlike structures with a random distribution and an average size of 500 nm (Figure 4C). However, TEM analysis showed that 40 nm uniformly shaped granular particles formed after Cu adsorption. Adsorbed Cu was present with these particles, demonstrating the growth of TiO_2 crystals on the surface (Figure 4D).

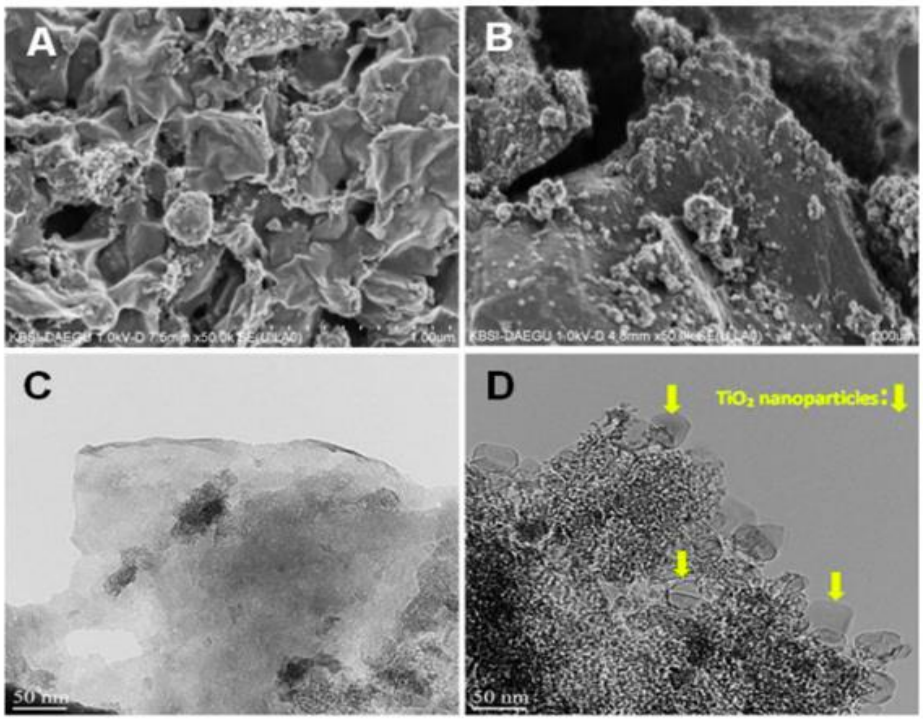

Figure 4. A, B) SEM and C, D) TEM images of 2D $Ti_3C_2T_x$ before and after Cu^{+2} adsorption [113] Copyright (2017) American Chemical Society

FTIR analysis

When MXenes are used as adsorbents, FT-IR examination reveals distinctive peaks that shed light on how dye molecules interact with the MXene surface. O-H stretching vibrations (3200-3600 cm^{-1}) for hydroxyl groups or adsorbed water molecules, C=O stretching vibrations (1700-1750 cm^{-1}) for carbonyl groups in MXenes or adsorbed dye molecules, and C-O stretching vibrations (1000-1200 cm^{-1}) for C–O bonds are some of the peaks in the FTIR spectra.

The functional groups involved in dye adsorption on MXene surfaces can be learned a lot from these peaks. The development of new chemical bonds between MXenes and dye molecules as well as changes in the makeup of functional groups can both be evaluated via FTIR analysis. Perumal Karthikeyan [114] reported the FTIR analysis of $Ti_3C_2T_x$ MXene being used as an adsorbent for Chromium and

methyl orange. He investigated that the -OH stretching vibrations of MXenes are thought to be the cause of the broadband at 3436 cm^{-1}. The H-OH stretching bands correlate to the unique peak at 1630 cm^{-1}, confirming the presence of the -OH group and water molecules on the surface of the absorbent. The existence of (=O), which is connected to the Ti-O-Ti vibrations, is specified by the vibration band at 865 cm^{-1}. Ti-C out-of-plane vibrations are represented by the characteristic peak at 615 cm^{-1} (Figure 5).

XPS

MXenes' XPS examination as dye adsorbents reveals information about their surface characteristics and chemical makeup. The material's numerous elements, including carbon (C1s), oxygen (O_1s), and transition metals (such as Ti_2p for titanium-based MXenes), are represented by the observed XPS peaks [115, 116].

These peaks' relative intensities, locations, and forms provide details about the MXene surface's chemical environment, bonding states, and surface functional groups. The interactions between the dye molecules adsorbed on the MXene surface are better understood thanks to this investigation. In a study by Byung Moon Jun [117] the composition of MXene and MOF as MB and AB-80 adsorbents is revealed by XPS studies. While MOF is made up of Al, C, and O components, the XPS spectra of MXene reveal the presence of Na, C, Ti, F, and O elements. The FTIR results are consistent with the lack of an N signal in the XPS spectra of MXene interacting with AB. In addition, there are variations in the N_1s peaks in the XPS spectra of MXene and MOF reacting with MB and AB.

Perhaps as a result of the strong bonding between the positive charge of MB and the negative charge of MXene, some of the MXene N_1s peak changes to the lower binding energy (Figure 6).

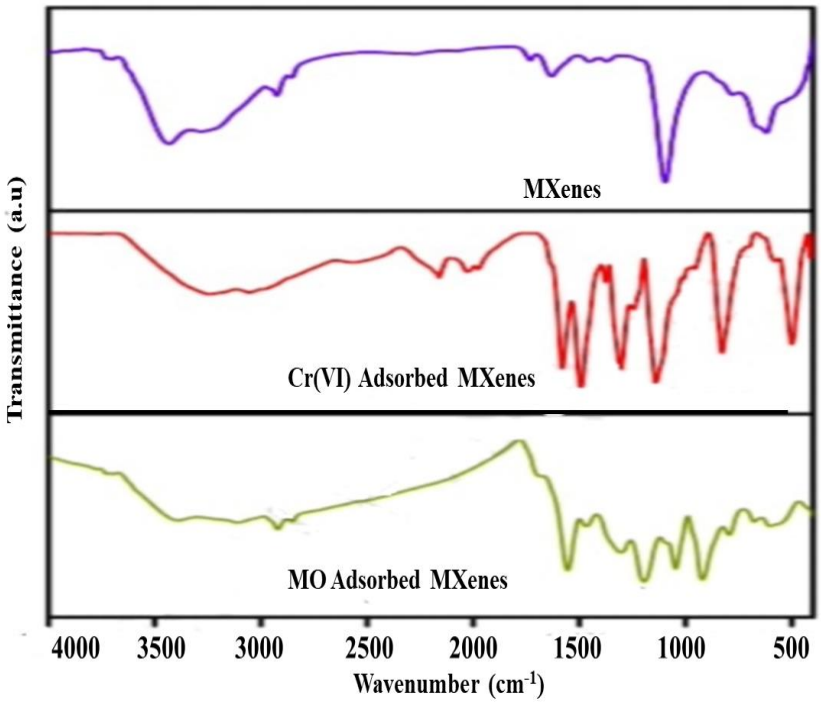

Figure 5. FT-IR spectra of MXenes for Cr and methyl orange [114] Copyright (2017) American Chemical Society

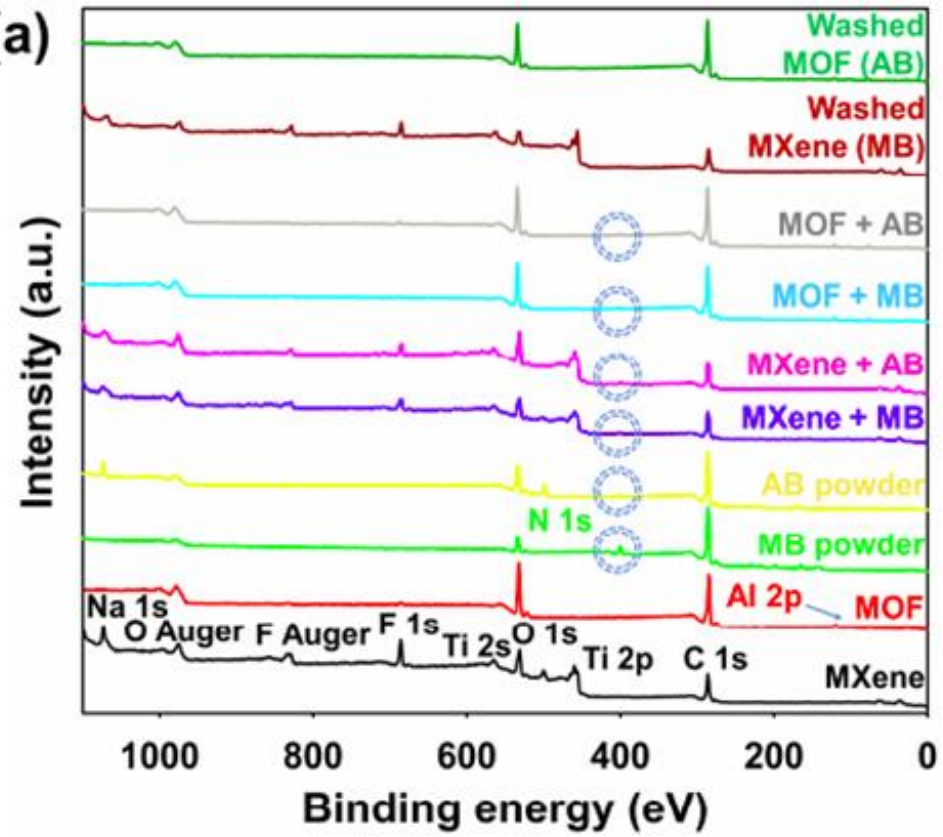

Figure 6. XPS spectra of MOF/MXene/MB/AB [117] Copyright (2020) American Chemical Society

Factors affecting MXene-dye adsorption

Effect of pH and surface charge

For dye to adhere to MXene materials, the pH of the solution is essential. PZC (point of zero charges) helps to understand the suitable pH for MXenes for dye adsorption [118]. Surface functional groups on MXenes are pH-sensitive and change from positively charged at low pH (acidic) to negatively charged at high pH (alkaline). The electrostatic interactions between dye molecules and MXene are controlled by its surface charge. Negatively charged MXene interacts favorably with anionic dyes while positively charged MXene attracts cationic dyes [119, 120]. Sehyeong Lim *et al.* [121] in their study investigated the effect of pH change on the adsorption efficiency of various dyes on the surface of Ti_3C_2 MXenes. As a whole, the charge type of the organic dye corresponded with the variation trends of the removal efficiencies versus pH. The removal efficiency of the anionic dyes (CR, MR, MO, and OG) and cationic dyes (MB and MV) changed as the pH rose and climbed, respectively. However, the apparent opposite pH dependence of the removal efficiencies for cationic and anionic dyes suggested the significance of the electrostatic interactions between the dyes and MXenes, which should be related to the charging states of the interacting species. The ubiquitous Van der Waals interactions undoubtedly played a role in the adsorption of all dyes. The efficiency oe removal of mxenes with different dyes is shown in the Figure 7.

Effect of contact time

On dye adsorption onto MXenes, contact time has a considerable impact. Due to the abundance of surface sites, dye molecules first bond to the MXene surface quickly. During this stage, the dye solution and MXene surface are in equilibrium. The adsorption capacity achieves a plateau with increasing contact duration, indicating saturation of the MXene surface. The influence of additional contact time on adsorption efficiency is constrained, indicating equilibrium. Models like pseudo-first-order or pseudo-second-order kinetics can be used to analyze how the kinetics of dye adsorption change with the length of the contract period. These models help in figuring out the ideal contact time for efficient dye removal as well as in understanding the adsorption mechanism [122, 123].

In a study by Jia Yan [124], it was found that increasing the time of contact increases the adsorption capacity for basic red 46 onto the surface of citric acid-alkalized Ti_3C_2 composite. The maximum adsorption capacity was 230.95 mg/g for 60 min.

Effect of adsorbent dosage

The dosage of the adsorbent or the amount of MXene material employed has a big impact on how well the dye is removed. By creating more binding sites on the MXene surface as a result of the increased dosage, the adsorption capacity and efficiency are improved. A faster and more efficient adsorption is made possible by the dye solution's steeper concentration gradient relative to the adsorbent surface.

There is, however, a dosage that works best, and subsequent augmentation may not considerably enhance adsorption capacity [125, 126].

Beyond this threshold, the further adsorbent may increase costs without commensurate increases in efficiency. To accomplish successful dye removal, maximize adsorption capacity, and take cost-effectiveness and material availability into account, the ideal dosage should be determined through experimental research [127]. Yafei Yan [128] reported that 1g·L^{-1} dose of adsorbent Nb_2CT_x is required to adsorb the maximum amount of MB and MO as 496 mg/g and 493 mg/g, respectively.

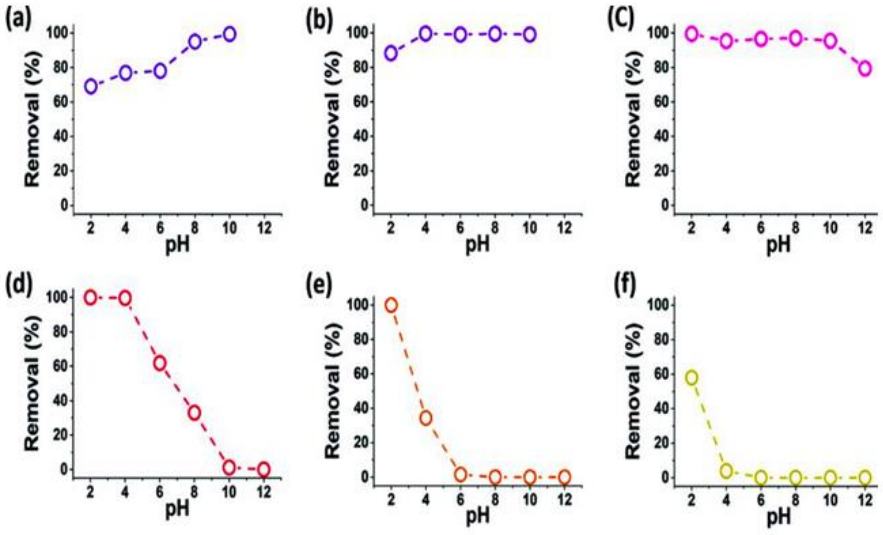

Figure 7. The MXene efficiency for removal of the following dyes: a) MB, b) MV, c) CR, d) MR, e) MO, and f) OG in batch adsorption studies carried out at various pH levels for 1 h [121]

Effect of temperature

The potential and general effectiveness of dye adsorption on MXenes are both significantly influenced by temperature. The adsorption capacity increases as temperature rises because dye molecules migrate and diffuse more readily toward the MXene surface [129]. Due to thermodynamic equilibrium, higher temperatures also encourage desorption from the solution and subsequent adsorption onto the MXene surface. The temperature effect can be influenced by variables including dye qualities and MXene properties. The solubility or stability of certain dyes may vary with temperature, whereas MXenes' thermal stability is essential for maintaining adsorption efficiency. Understanding how temperature affects adsorption enables the use of MXene-based adsorbents to optimize the adsorption procedure for effective dye removal [130]. A study by Xuemei Wang *et al.* [131] revealed that according to statistical physical and thermodynamic investigations, receptor density (Dm) played a major role in the reversible endothermic adsorption process that drove the adsorption of MB and CR onto MCF. The high temperature was advantageous to the occurrence of high adsorption capacity on the surface of MXene/carbon foam hybrid aerogel. Dan Liu [132] claimed that the value of ΔH^{o} demonstrated endothermic DOX adsorption onto the Ti_3C_2@Fe_3O_4@-CD and an increase in DOX adsorption percentage with temperature. The negative values of ΔG^{o} suggested that the DOX adsorption process onto the Ti_3C_2@Fe_3O_4@-CD was a viable and spontaneous process, while the value of ΔS^{o} indicated a higher order of the reaction (Table 3).

Overview of data in tabulated form

Table 4 presents a thorough review of the MXenes-based adsorption of different colors from water. The information in the table shows how well MXenes work to get rid of dyes and gives useful details on each dye's adsorption capability and efficiency.

Regeneration and recyclability of adsorbent

For their practical application and environmental sustainability, MXene adsorbents used for dye adsorption should be regenerative and recyclable. To reuse dye-loaded MXene adsorbents, various techniques have been used to recover their adsorption ability [137]. To encourage the desorption of dyes that have been absorbed, thermal regeneration entails heating the adsorbents. To specifically desorb the dyes from the adsorbent surface, chemical regeneration employs regenerants such as acids, alkalis, organic solvents, or complexing agents [138, 139]. Selectivity and *in situ* regeneration are two benefits of electrochemical regeneration, which uses an electrical potential to promote desorption. These procedures can be carried out in batch systems where the regenerant solution and dye-loaded adsorbents are combined and adequate desorption conditions are maintained. Based on the extent of dye removal and the restoration of adsorption capacity, the regeneration's efficacy is assessed. MXene adsorbents' long-term viability as sustainable and affordable solutions for dye removal applications is largely attributed to their successful regeneration and recyclability [140, 141]. Chong Cai [135] revealed that after the initial dye adsorption test, MXene nanocomposites underwent several items of washing with ethanol and water. Additional dye adsorption studies with MB and RhB were then carried out for 12 cycles. According to the experimental findings,

Table 3. Thermodynamic conditions for DOX adsorption on Ti_3C_2@Fe_3O_4@-CD [132]

Temperature (K)	ΔG° (KJ/mol)	ΔH° (KJ/mol)	ΔS° (J/mol/K)
308	-3.19	-	-
298	-2.68	11.63	48.05
318	-3.63	-	-

Table 4. Summary of dyes adsorption by MXenes

Mxene	Dyes	pH	Temperature	Contact time	Removal efficiency	References
PAC-MXene	Safranine T	-	298 k	-	36.76 mg/g	[133]
PAC-MXene	Neutral Red	-	298 k	-	42.50 mg/g	[133]
LiOH- Ti_3C_2Tx	MB	9	25 °C	20 min	121 mg.g	[134]
NaOH-Ti_3C_2Tx	MB	8.8-9	25 °C	20 min	189 mg/g	[134]
Phytic acid-MXene	MB	10	25 °C	18 min	42 mg/g	[135]
Phytic acid-MXene	Rh. B	11.5	25 °C	18 min	22 mg/g	[135]
MXene/PEI/sodium alginate aerogel	Congo Red	3	-	-	3568 mg/g	[136]
Ti_3C_2Tx MXene nanosheets	MO	<6	-	40 min	94.8 mg/g	[114]

the PA-MXene-12 composite's MB adsorption capacity was maintained at about 85% after 12 continuous cycles as opposed to 98% during the initia adsorption phase. Similar results were observed with RhB, where the composite preserved around 84% of its initial 97% adsorption capacity after 12 consecutive cycles. Based on these results, it can be concluded that the PA-MXene composites showed good repeatability and stability during the adsorption cycles.

Adsorption mechanism

MXene adsorption depends on electrostatic interactions. Functional groups or flaws frequently cause MXene surfaces to have a net charge. Depending on the charges of the dye molecules, the MXene surface charge attracts or repels them. Negatively charged dye molecules are drawn to positive MXene surfaces and vice versa. On the MXene surfaces, the dye binds to this attraction. MXenes and dyes have similar surface charges, which may prevent adsorption. To maximize dye adsorption and managing capacity on MXenes, it is essential to comprehend electrostatic interactions and surface charge effects [142-144]. It is seen that at pH values above 8, 6, and 4, respectively, the removal efficiencies of the MXenes for MR, MO, and OG are nearly zero, indicating that the adsorption of these anionic dyes in these pH ranges is minimal [145].

Van der Waals forces and π-π stacking also play significant roles in MXene adsorption. When aromatic dye molecules interact with the aromatic structures of MXene, π-π stacking takes place, leading to powerful dye-MXene interactions through overlapping π-electron clouds [146]. Adsorption is further influenced by Van der Waals forces, including dipole-dipole interactions and London dispersion forces. The MXene surface and dye molecules are made to interact weakly thanks to these forces, which increases the adsorption capacity overall. MXenes are effective adsorbents for dye removal because of the combined effect of π-π

stacking and van der Waals forces, which facilitate efficient dye adsorption them [147-149]. Zhengguo Wu [150] in his study showed that physical adsorption is responsible for crystal violet dye and MXene/Carbon microspheres. Interactions were found to be H-bonding, interactions, electrostatic interactions, and π-π stacking.

Furthermore, adsorption is impacted by functional groups and surface flaws on MXenes. MXene surfaces are modified by hydroxyl (-OH), carboxyl (-COOH), and amino (-NH2) groups, enabling particular interactions with dye molecules. Through complexation, electrostatic interactions, or hydrogen bonds, these groups operate as the dye's active adsorption sites. Additional adsorption sites are provided by surface flaws like oxygen or vacancy vacancies, which also change the electronic characteristics of MXene and aid in the adsorption process. The capacity, selectivity, and efficacy of MXenes as dye removal adsorbents are enhanced by the presence of functional groups and surface imperfections [151-153].

The adsorption of dyes on MXenes involves both physical and chemical adsorption mechanisms. While chemical adsorption involves more robust connections and produces more persistent adsorption, physical adsorption is primarily controlled by weak intermolecular forces and is irreversible. Both physical and chemical adsorption are affected by factors like electrostatic interactions, surface charge effects, π-π stacking, Van der Waals forces, functional groups, and surface defects. These factors affect the strength and nature of the interactions between MXenes and dye molecules [154, 155]. The possible mechanism of some of the dyes on MXenes is depicted in Figure 8.

Challenges and limitations of MXenes as dye removal adsorbent

The low selectivity of MXenes as dye removal adsorbents is one of their main drawbacks. Due to their huge surface areas, MXenes may efficiently bind various dyes through hydrogen bonds and electrostatic interactions. While this adaptability may be helpful in some circumstances, it can also result in indiscriminate adsorption, which lowers selectivity. This restriction may make it more difficult to effectively remove particular colors or target contaminants from intricate wastewater matrices [156, 157].

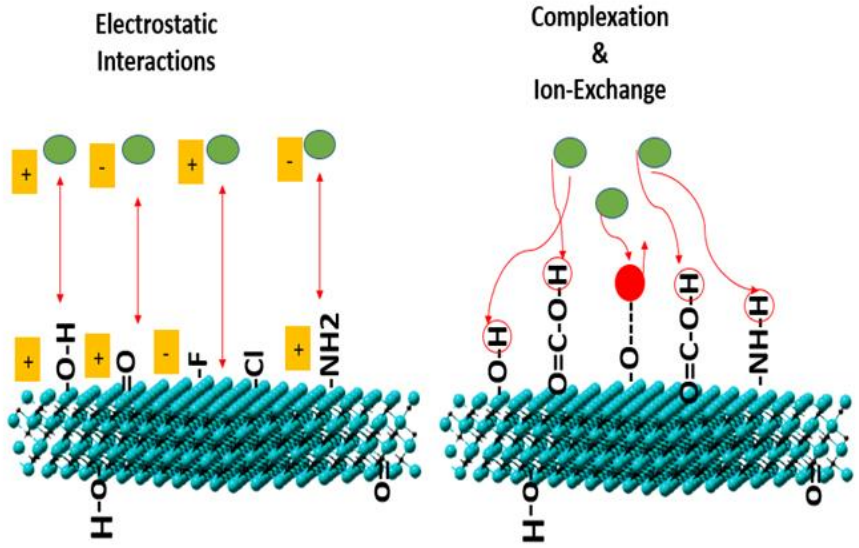

Figure 8. Adsorption mechanism of some dyes on MXenes

The tendency of MXene nanosheets to aggregate presents another difficulty. MXenes frequently have high surface energies and a propensity to agglomerate, which may make them less accessible to dye molecules and lower their ability for adsorption. The stability and reusability of MXenes as adsorbents can both be impacted by aggregation.

The creation of aggregation prevention or mitigation techniques, such as surface functionalization or composite production with appropriate support materials, is necessary to get around this restriction [158, 159].

Moreover, Practical difficulties arise from MXenes' capacity to regenerate and be reused as adsorbents. While MXenes can be recovered via desorption methods such as solvent extraction or thermal treatment, these procedures are not always effective or ecologically friendly. Some dyes may interact with MXene surfaces intensely, making it difficult to remove them. In addition, repeated regeneration cycles may cause the MXene structure to deteriorate or vanish, which will reduce the effectiveness of its adsorption. Research is still being done to find efficient and long-lasting ways to regenerate MXenes without reducing their adsorption capacity [160, 161].

However, the MXenes surface can be altered using a variety of techniques, providing an opportunity to vary their characteristics for certain dye removal applications. The most crucial one is surface modification techniques. Through electrostatic or -interactions, functionalization with organic molecules like amino, carboxyl, or hydroxyl groups improves adsorption. In addition, functionalization increases stability and dispersibility while minimizing aggregation tendencies and increasing surface area. MXene-polymer-nanoparticle-zeolite composite materials produce synergistic adsorption systems that improve capacity and selectivity. Surface roughness or hierarchical structures increase the number of active sites for dye adsorption and change the surface charge distribution, which facilitates selective adsorption [162-164].

Conclusion

MXenes have a particular edge over nanoparticles and nanocomposites when it comes to dye absorption because of their special mix of high surface area, variable surface chemistry, and superior electrical conductivity. Their layered structure offers many adsorption sites for dye molecules, and by functionalizing them, their surface chemistry can be modified to improve dye binding. Due to the high electrical conductivity of MXenes, dye degradation can be accelerated through photocatalysis and electrochemistry. Furthermore, their resilience to different environmental factors guarantees continued functioning. Compared to the traditional nanoparticles and nanocomposites, these characteristics make MXenes an attractive alternative for effective and adaptable dye removal and degradation. In a nutshell, MXenes, due to their special qualities and numerous surface modification procedures, hold a lot of promise as adsorbents for dye removal. They provide more binding sites and customized interactions with dyes, improving their overall performance. MXenes play a vital role in alleviating the problems associated with water contamination by providing a long-lasting and affordable remedy. They are adaptable to different dye kinds, regenerate and reuse, and have the capacity to scale. MXenes need to be optimized, innovative surface modifications explored, their adsorption methods clarified, and their behavior in intricate wastewater matrices investigated. Studies on long-term stability, cost-effectiveness, and scalability are also essential. MXenes have the potential for applications other than dye removal, which

justifies further investigation. Their full potential in water treatment and environmental remediation will be realized with continued research and development efforts.

Acknowledgments

The authors acknowledge the Chemistry Department, University of Wah, Quaid Avenue, Wah Cantt., (47010), Punjab, Pakistan for supporting this work.

Disclosure Statement

No potential conflict of interest was reported by the authors.

Funding

This research did not receive any specific grant from funding agencies in the public, commercial, or not-for-profit sectors.

Authors' Contributions

All authors contributed to data analysis, drafting, and revising of the paper and agreed to be responsible for all the aspects of this work.

Orcid

Farhad Ali
https://orcid.org/0009-0005-0374-7534
Shafaq Zahid
https://orcid.org/0009-0004-7912-4854
Shakir Khan
https://orcid.org/0009-0001-9735-0140
Shafi Ur Rehman
https://orcid.org/0000-0003-2370-6498
Fawad Ahmad
https://orcid.org/0000-0003-2404-5572

References

[1]. Nagar A., Pradeep T. *ACS Nano*., 2020, **14**:6420 [Crossref], [Google Scholar], [Publisher]
[2]. Huang L., Huang X., Yan J., Liu Y., Jiang H., Zhang H., Tang J., Liu Q. *J Hazard Mater*., 2023, **442**:130024 [Crossref], [Google Scholar], [Publisher]
[3]. Pranta J.B., Chakraborty P., Hossain N. In *Emerging Technologies in Applied and Environmental Microbiology.,* 2023, 1 [Crossref], [Google Scholar], [Publisher]
[4]. Happel A., Gallagher D. *Sci Total Environ*., 2022, **824**:153776 [Crossref], [Google Scholar], [Publisher]
[5]. Vena N.B. *J Plan Hist*., 2022, **21**:249 [Crossref], [Google Scholar], [Publisher]
[6]. Xu H., Gao Q., Yuan B. *Ecol Indic*., 2022, **135**:108561 [Crossref], [Google Scholar], [Publisher]
[7]. Fida M., Li P., Wang Y., Alam S.K., Nsabimana A. *Expos. Health*., 2023, **15**:619 [Crossref], [Google Scholar], [Publisher]
[8]. Xue J., Wang Q., Zhang M. *Sci Total Environ*., 2022, **826**:154146 [Crossref], [Google Scholar], [Publisher]
[9]. a) kidwai M., Dwivedi P., Jahan A. *Journal of Applied Organometallic Chemistry*, 2023, **3**:156 [Crossref], [Publisher]; b) Patil N., Shinde D., Patil P. *Journal of Applied Organometallic Chemistry*, 2023, **3**:1 [Crossref], [Publisher]
[10]. Taghavi Fardood S., Moradnia F., Heidarzadeh S., Naghipour A. *Nanochem Res*., 2023, **8**:134 [Crossref], [Google Scholar], [Publisher]
[11]. Moradnia F., Fardood S.T., Ramazani A., Gupta V.K. *J. Photochem. Photobiol. A: Chem*., 2020, **392**:112433 [Crossref], [Google Scholar], [Publisher]
[12]. El Bilali A., Lamane H., Taleb A., Nafii A. *J. Clean. Prod*., 2022, **368**:133227 [Crossref], [Google Scholar], [Publisher]
[13]. Moradnia F., Fardood S.T., Ramazani A., Min B.-k., Joo S.W., Varma R.S. *J. Clean. Prod*., 2021, **288**:125632 [Crossref], [Google Scholar], [Publisher]

[14]. Swami M.B., Nagargoje G.R., Mathapati S.R., Bondge A.S., Jadhav A.H., Panchgalle S.P., More V. *Journal of Applied Organometallic Chemistry*, 2023, **3**:184 [Crossref], [Publisher]
[15]. Emmanuel S.S., Adesibikan A.A., Saliu O.D. *Appl. Organomet. Chem*., 2023, **37**:e6946 [Crossref], [Google Scholar], [Publisher]
[16]. Islam T., Repon M.R., Islam T., Sarwar Z., Rahman M.M. *Environ. Sci. Pollut. Res*., 2023, **30**:9207 [Crossref], [Google Scholar], [Publisher]
[17]. Verma N., Chundawat T.S., Chandra H., Vaya D. *Mater. Res. Bull*., 2023, **158**:112043 [Crossref], [Google Scholar], [Publisher]
[18]. Madhusudhana N., Yogendra K., Veena S., Varsha G.k. 2022, **8** [Google Scholar], [Publisher]
[19]. Senguttuvan S., Senthilkumar P., Janaki V., Kamala-Kannan S. *Chemosphere*., 2021, **267**:129201 [Crossref], [Google Scholar], [Publisher]
[20]. Hussain B., Yaseen H., Al-Misned F., Qasim M., Al-Mulhm N., Mahboob S. *Saudi J. Biol. Sci*., 2021, **28**:2267 [Crossref], [Google Scholar], [Publisher]
[21]. Kishor R., Purchase D., Saratale G.D., Saratale R.G., Ferreira L.F.R., Bilal M., Chandra R., Bharagava R.N. *J. Environ. Chem. Eng.*, 2021, **9**:105012 [Crossref], [Google Scholar], [Publisher]
[22]. Vats S., Srivastava S., Maurya N., Saxena S., Mudgil B., Yadav S., Chandra R. *Biological Approaches to Controlling Pollutants*., 2022, 139 [Crossref], [Google Scholar], [Publisher]
[23]. a) Das S., Singh S., Garg S. *Orient. J. Chem*., 2019, **35** [Google Scholar], [Publisher]; b) Rostamzadeh Mansour S., Sohrabi-Gilani N., Nejati P. *Advanced Journal of Chemistry, Section A*, 2022, **5**:31 [Crossref], [Publisher]; c) Sanati M., Dehno Khalaji A., Mokhtari A., Keyvanfard M. *Prog. Chem. Biochem. Res*., 2021, **4**:319 [Crossref], [Publisher]; d) Sanad Akrab S., Jasim Mohammed A. *J. Med. Pharm. Chem. Res*., 2023, **5**:63 [Publisher]; e) Sarathi R., Renuga Devi L., Sheeba N.L., Selva Esakki E., Meenakshi Sundar S. *J. Chem. Rev*., 2023, **5**:15 [Crossref], [Publisher]; f) Mahmoodiyeh B., Taleby H., Etemadi S., Sadri M.S., Susanabadi A., Milani Fard M. *Journal of Chemical Reviews*, 2021, **3**:219 [Crossref], [Publisher]; g) Mousavi Ghahfarokhi S.E., Helfi K., Zargar Shoushtari M. *Advanced Journal of Chemistry, Section A*, 2022, **5**:45 [Crossref], [Publisher]; h) Satar Kazem M., Mohammed Abbas A. *J. Med. Pharm. Chem. Res*., 2022, **4**:1218 [Publisher]; i) Ahmed M., Dekhyl A., Alwan L. *J. Med. Pharm. Chem. Res*., 2022, **4**:852 [Publisher]; j) Khalid Hamood Al-Behadili W., M. Jawad Y., Hasan H.J. *Asian Journal of Green Chemistry*, 2023, **7**:163 [Crossref], [Publisher]; k) Eltaboni F., Bader N., El-Kailany R., Elsharif N., Ahmida A. *Journal of Chemical Reviews*, 2022, **4**:313 [Crossref], [Publisher]; l) Al-Mutlaq S., Mahal E. *J. Med. Pharm. Chem. Res.,* 2022, **4**:580 [Publisher]; m) Bashandeh Z., Dehno Khalaji A. *Advanced Journal of Chemistry, Section A*, 2021, **4**:270 [Crossref], [Publisher]; n) Chala G. *Journal of Chemical Reviews*, 2023, **5**:1 [Crossref], [Publisher]
[24]. a) Sonal S., Mishra B.K. *Water pollution and management practices*., 2021, 303 [Crossref], [Google Scholar], [Publisher]; b) M. Abdul Hassan M., S. Hassan S., K. Hassan A. *J. Med. Pharm. Chem. Res*., 2022, **4**:1062 [Publisher]; c) Belhadri M., Mokhtar A., Bengueddach A., Sassi M. *J. Med. Pharm. Chem. Res*., 2021, **3**:881 [Publisher]; d) Ullah R. *Journal of Chemical Reviews*, 2023, **5**:466 [Crossref], [Publisher]; e) Ghanavati B., Bozorgian A., Kazemi Esfeh H. *Prog. Chem. Biochem. Res*., 2022, **5**:165 [Crossref], [Publisher]; f) Bashandeh Z., Dehno Khalaji A. *Journal of Medicinal and Nanomaterials Chemistry*, 2023, **5**:243 [Crossref], [Publisher]; g) Dessie Y., Tadesse S. *Journal of Chemical Reviews*, 2021, **3**:320 [Crossref], [Publisher]; h) Ali F., Fazal S., Iqbal N., Zia A., Ahmad F. Journal of Medicinal and

Nanomaterials Chemistry, 2023, 5:106 [Crossref], [Publisher]; f) Aboshaloa E., Asweisi A., Almusrati A., Almusrati M., Aljhane H. *Journal of Medicinal and Nanomaterials Chemistry*, 2022, **4**:234 [Crossref], [Publisher]; i) Mohammed Alkherraz A., Elsherif K.M., El-Dali A., Blayblo N.A., Sasi M. *Journal of Medicinal and Nanomaterials Chemistry*, 2022, **4**:118 [Crossref], [Publisher]; j) Mohammed Z., Jasim Mohammed A. *J. Med. Pharm. Chem. Res*., 2023, **5**:73 [Publisher]; k) Al-Asadi S., Al-Qaim F. *J. Med. Pharm. Chem. Res*., 2023, **5**:794 [Crossref], [Google Scholar], [Publisher]

[25]. a) Khalid N., Kalsoom U., Ahsan Z., Bilal M. *Int. J. Biol. Macromol*., 2022, **207**:387 [Crossref], [Google Scholar], [Publisher]; b) AL-Mammar D. *J. Med. Pharm. Chem. Res*., 2022, **4**:175 [Publisher]; c) Muhi-Alden Y., Saleh K. *J. Med. Pharm. Chem. Res*., 2021, **3**:755 [Publisher]; d) Akeremale O. *Journal of Chemical Reviews*, 2022, 4:1 [Crossref], [Publisher]; e) Dehno Khalaji A., Machek P., Jarosova M. *Advanced Journal of Chemistry, Section A*, 2021, **4**:317 [Crossref], [Publisher]

[26]. Ihaddaden S., Aberkane D., Boukerroui A., Robert D. *JWPE*., 2022, **49**:102952 [Crossref], [Google Scholar], [Publisher]

[27]. Ihaddaden S., Aberkane D., Boukerroui A., Robert D. *JWPE*., 2022, **49**:102952 [Crossref], [Google Scholar], [Publisher]

[28]. Pervez M.N., Stylios G.K., Liang Y., Ouyang F., Cai Y. *J. Clean. Prod*., 2020, **262**:121301 [Crossref], [Google Scholar], [Publisher]

[29]. Haounati R., Ighnih H., Malekshah R.E., Alahiane S., Alakhras F., Alabbad E., Alghamdi H., Ouachtak H., Addi A.A., Jada A. *Mater. Today Commun*., 2023, **35**:105915 [Crossref], [Google Scholar], [Publisher]

[30]. Jankowska K., Su Z., Zdarta J., Jesionowski T., Pinelo M. *J. Hazard. Mater*., 2022, **435**:129071 [Crossref], [Google Scholar], [Publisher]

[31]. Oladoye P.O., Ajiboye T.O., Wanyonyi W.C., Omotola E.O., Oladipo M.E. *Sustain. Chem. Enviorn*., 2023, 100033 [Crossref], [Google Scholar], [Publisher]

[32]. Qazi U.Y., Iftikhar R., Ikhlaq A., Riaz I., Jaleel R., Nusrat R., Javaid R. *Environ. Sci. Pollut. Res*., 2022, **29**:89485 [Crossref], [Google Scholar], [Publisher]

[33]. Ajormal F., Moradnia F., Taghavi Fardood S., Ramazani A. *J. Chem. Rev*., 2020, **2**:90 [Google Scholar], [Publisher]

[34]. Taghavi Fardood S., Moradnia F., Ramazani *Micro & Nano Letters,* 2019, **14**:986 [Crossref], [Google Scholar], [Publisher]

[35]. Moradnia F., Ramazani A., Fardood S.T., Gouranlou F. *MRX*., 2019, **6**:075057 [Google Scholar], [Publisher]

[36]. Taghavi Fardood S., Moradnia F., Moradi S., Forootan R., Yekke Zare F., Heidari M. *Nanochem Res*., 2019, **4**:140 [Google Scholar], [Publisher]

[37]. Kalam S., Abu-Khamsin S.A., Kamal M.S., Patil S. *ACS omega*., 2021, **6**:32342 [Crossref], [Google Scholar], [Publisher]

[38]. Li X., Zhang L., Yang Z., Wang P., Yan Y., Ran J. *Sep. Purif. Technol*., 2020, **235**:116213 [Crossref], [Google Scholar], [Publisher]

[39]. Zhao X., Zheng M., Gao X., Zhang J., Wang E., Gao Z. *Coord. Chem. Rev*., 2021, **440**:213970 [Crossref], [Google Scholar], [Publisher]

[40]. Mariyam A., Shahid M., I M., Khan M.S., Ahmad M.S. *J. Inorg. Organomet. Polym. Mater*., 2020, **30**:1935 [Crossref], [Google Scholar], [Publisher]

[41]. Hao M., Liu Y., Wu W., Wang S., Yang X., Chen Z., Tang Z., Huang Q., Wang S., Yang H. Wang X., *Energy Chem*., 2023, 100101 [Crossref], [Google Scholar], [Publisher]

[42]. Sajid M., Asif M., Baig N., Kabeer M., Ihsanullah I., Mohammad A.W. *JWPE*., 2022, **47**:102815 [Crossref], [Google Scholar], [Publisher]

[43]. Manea Y.K., Khan A.M., Wani A.A., Saleh M.A.S., Qashqoosh M.T.A., Shahadat M., Rezakazemi M. *J. Environ. Chem. Eng*., 2022, **10**:106848 [Crossref], [Google Scholar], [Publisher]
[44]. Arora B., Attri P. *J. Compos. Sci*., 2020, **4**:135 [Crossref], [Google Scholar], [Publisher]
[45]. Zhang H., Chhowalla M., Liu Z. *Chem Soc Rev*., 2018, **47**:3015 [Crossref], [Google Scholar], [Publisher]
[46]. Fan X., Li S., Zhang W., Xu W. *Ceram. Int*., 2023, **49**:5559 [Crossref], [Google Scholar], [Publisher]
[47]. Alimohammadi F., Sharifian Gh M., Attanayake N.H., Thenuwara A.C., Gogotsi Y., Anasori B., Strongin D.R. *Langmuir*., 2018, **34**:7192 [Crossref], [Google Scholar], [Publisher]
[48]. Kumar R., Sahoo S., Joanni E., Shim J.J. *Compos. B: Eng*., 2023, 110874 [Crossref], [Google Scholar], [Publisher]
[49]. Ronchi R.M., Arantes J.T., Santos S.F. *Ceram. Int*., 2019, **45**:18167 [Crossref], [Google Scholar], [Publisher]
[50]. Khazaei M., Mishra A., Venkataramanan N.S., Singh A.K., Yunoki S. *Curr Opin Solid State Mater Sci*., 2019, **23**:164 [Crossref], [Google Scholar], [Publisher]
[51]. Sajid M. *Anal. Chim. Acta*., 2021, **1143**:267 [Crossref], [Google Scholar], [Publisher]
[52]. Guo X., Zhang X., Zhao S., Huang Q., Xue J. *Phys. Chem. Chem. Phys*., 2016, **18**:228 [Crossref], [Google Scholar], [Publisher]
[53]. Lei Y., Cui Y., Huang Q., Dou J., Gan D., Deng F., Liu M., Li X., Zhang X., Wei Y. *Ceram. Int*., 2019, **45**:17653 [Crossref], [Google Scholar], [Publisher]
[54]. Firouzjaei M.D., Karimiziarani M., Moradkhani H., Elliott M., Anasori B. *Mater. Today Adv*., 2022, **13**:100202 [Crossref], [Google Scholar], [Publisher]
[55]. Naguib M., Barsoum M.W., Gogotsi Y. *Adv. Mater*., 2021, **33**:2103393 [Crossref], [Google Scholar], [Publisher]
[56]. Zhou A., Liu Y., Li S., Wang X., Ying G., Xia Q., Zhang P. *J. Adv. Ceram*., 2021, **10**:1194 [Crossref], [Google Scholar], [Publisher]
[57]. Kim Y.J., Kim S.J., Seo D., Chae Y., Anayee M., Lee Y., Gogotsi Y., Ahn C.W., Jung H.T. *Chem. Mater*., 2021, **33**:6346 [Crossref], [Google Scholar], [Publisher]
[58]. Ajmal S., Kumar A., Selvaraj M., Alam M.M., Yang Y., Das D.K., Gupta R.K., Yasin G. *Coord. Chem. Rev*., 2023, **483**:215094 [Crossref], [Google Scholar], [Publisher]
[59]. Peera S.G., Liu C., Shim J., Sahu A.K., Lee T.G., Selvaraj M., Koutavarapu R. *Ceram. Int*., 2021, **47**:28106 [Crossref], [Google Scholar], [Publisher]
[60]. Lin S., Hu X., Lin J., Wang S., Xu J., Cai F., Lin J. *Analyst*., 2021, **146**:4391 [Crossref], [Google Scholar], [Publisher]
[61]. Dong H., Yang W., Sun A., Zhan Y., Chen Y., Chen X. *High Perform. Polym*., 2023, **35**:181 [Crossref], [Google Scholar], [Publisher]
[62]. Lamiel C., Hussain I., Warner J.H., Zhang K. *Mater Today*., 2023, **63**:313 [Crossref], [Google Scholar], [Publisher]
[63]. Li Y., Shao H., Lin Z., Lu J., Liu L., Duployer B., Persson P.O., Eklund P., Hultman L., Li M. *Nat. Mater*., 2020, **19**:894 [Crossref], [Google Scholar], [Publisher]
[64]. Lin Y.C., Torsi R., Younas R., Hinkle C.L., Rigosi A.F., Hill H.M., Zhang K., Huang S., Shuck C.E., Chen C., Lin Y.H., Maldonado-Lopez D., Mendoza-Cortes J.L., Ferrier J., Kar S., Nayir N., Rajabpour S., van Duin A.C.T., Liu X., Jariwala D., Jiang J., Shi J., Mortelmans W., Jaramillo R., Lopes J.M.J., Engel-Herbert R., Trofe A., Ignatova T., Huat Lee S., Mao Z., Damian L., Wang Y., Steves M.A., Knappenberger Jr K.L., Wang Z., Law S., Bepete G., Zhou D., Lin J.X., Scheurer M.S., Li J., Wang P., Yu G., Wu S., Akinwande D., Redwing J.M., Terrones M., Robinson J.A. *ACS nano*., 2023,

17:9694 [Crossref], [Google Scholar], [Publisher]
[65]. Mao M., Yu K.X., Cao C.F., Gong L.X., Zhang G.D., Zhao L., Song P., Gao J.F., Tang L. *J. Chem. Eng*., 2022, **427**:131615 [Crossref], [Google Scholar], [Publisher]
[66]. Yakusheva A., Saranin D., Muratov D., Gostishchev P., Pazniak H., Di Vito A., Le T.S., Luchnikov L., Vasiliev A., Podgorny D. *Small*., 2022, **18**:2201730 [Crossref], [Google Scholar], [Publisher]
[67]. Xuan J., Wang Z., Chen Y., Liang D., Cheng L., Yang X., Liu Z., Ma R., Sasaki T., Geng F. *Angew. Chem*., 2016, **128**:14789 [Crossref], [Google Scholar], [Publisher]
[68]. Li G., Tan L., Zhang Y., Wu B., Li L. *Langmuir*., 2017, **33**:9000 [Crossref], [Google Scholar], [Publisher]
[69]. Shahzad F., Zaidi S.A., Naqvi R. *Crit Rev Anal Chem*., 2022, **52**:848 [Crossref], [Google Scholar], [Publisher]
[70]. Anasori B., Naguib M., Bulletin G.E.J.M. 2023, **48**:238 [Crossref], [Publisher]
[71]. Sun W., Shah S., Chen Y., Tan Z., Gao H., Habib T., Radovic M., Green M. *J. Mater. Chem. A*., 2017, **5**:21663 [Crossref], [Google Scholar], [Publisher]
[72]. Pang S.-Y., Wong Y.-T., Yuan S., Liu Y., Tsang M.-K., Yang Z., Huang H., Wong W.-T., Hao J. *J. Am. Chem. Soc*., 2019, **141**:9610 [Crossref], [Google Scholar], [Publisher]
[73]. Firestein K.L., von Treifeldt J.E., Kvashnin D.G., Fernando J.F., Zhang C., Kvashnin A.G., Podryabinkin E.V., Shapeev A.V., Siriwardena D.P., Sorokin P. *Nano Lett*., 2020, **20**:5900 [Crossref], [Google Scholar], [Publisher]
[74]. Zhou H., Zhou Y., Cao Y., Wang Z., Wang J., Zhang Y., Pan W. *J. Chem. Eng*., 2023, **461**:142035 [Crossref], [Google Scholar], [Publisher]
[75]. Gu J., Zhao Z., Huang J., Sumpter B.G., Chen Z. *ACS nano*., 2021, **15**:6233 [Crossref], [Google Scholar], [Publisher]
[76]. Meng Q., Ma J., Zhang Y., Li Z., Zhi C., Hu A., Fan J. *Nanoscale*., 2018, **10**:3385 [Crossref], [Google Scholar], [Publisher]
[77]. Zou H., He B., Kuang P., Yu J., Fan K. *ACS Appl. Mater. Interfaces*., 2018, **10**:22311 [Crossref], [Google Scholar], [Publisher]
[78]. Wang G. *J. Phys. Chem. C*., 2016, **120**:18850 [Crossref], [Google Scholar], [Publisher]
[79]. Wang H., Cui H., Song X., Xu R., Wei N., Tian J., Niu H. *J. Colloid Interface Sci*., 2020, **561**:46 [Crossref], [Google Scholar], [Publisher]
[80]. Ng V.M.H., Huang H., Zhou K., Lee P.S., Que W., Xu J.Z., Kong L.B. *J. Mater. Chem. A*., 2017, **5**:3039 [Crossref], [Google Scholar], [Publisher]
[81]. Liu Z., Alshareef H.N.J. *Advanced Electronic Materials,* 2021, **7**:2100295 [Crossref], [Publisher]
[82]. Orts Mercadillo V., Chan K.C., Caironi M., Athanassiou A., Kinloch I.A., Bissett M., Cataldi P. *Adv. Funct. Mater*., 2022, **32**:2204772 [Crossref], [Google Scholar], [Publisher]
[83]. Fattahi M., Ezzatzadeh E., Jalilian R., Taheri A. *J HazardMater*., 2021, **403**:123716 [Crossref], [Google Scholar], [Publisher]
[84]. Zang X., Wang J., Qin Y., Wang T., He C., Shao Q., Zhu H., Cao N. *Nanomicro Lett*., 2020, **12**:1 [Crossref], [Google Scholar], [Publisher]
[85]. Kim H., Anasori B., Gogotsi Y., Alshareef H.N. *Chem. Mater*., 2017, **29**:6472 [Crossref], [Google Scholar], [Publisher]
[86]. He J., Liu S., Deng L., Shan D., Cao C., Luo H., Yan S. *Appl. Surf. Sci*., 2020, **504**:144210 [Crossref], [Google Scholar], [Publisher]
[87]. Tariq A., Ali S.I., Akinwande D., Rizwan S. *ACS omega*., 2018, **3**:13828 [Crossref], [Google Scholar], [Publisher]
[88]. Lipatov A., Lu H., Alhabeb M., Anasori B., Gruverman A., Gogotsi Y., Sinitskii A. *Sci adv*., 2018, **4**:eaat0491 [Crossref], [Google Scholar], [Publisher]
[89]. Borysiuk V.N., Mochalin V.N., Gogotsi Y. *Nanotechnol*., 2015, **26**:265705 [Google Scholar], [Publisher]

[90]. Zhang J., Kong N., Uzun S., Levitt A., Seyedin S., Lynch P.A., Qin S., Han M., Yang W., Liu J. *Adv Mater*., 2020, **32**:2001093 [Crossref], [Google Scholar], [Publisher]
[91]. Luo S., Patole S., Anwer S., Li B., Delclos T., Gogotsi O., Zahorodna V., Balitskyi V., Liao K. *Nanotechnol*., 2020, **31**:395704 [Google Scholar], [Publisher]
[92]. Gogotsi Y. *Matter*., 2022, **5**:381 [Google Scholar], [Publisher]
[93]. Liang B., Liao X., Zhu Q., Yu M., Li J., Geng B., Liu K., Jia D., Yang Z., Zhou Y. *Ceram. Int.*, 2021, **47**:27730 [Crossref], [Google Scholar], [Publisher]
[94]. Wu Z., Wei L., Tang S., Xiong Y., Qin X., Luo J., Fang J., Wang X. *ACS nano*., 2021, **15**:18880 [Crossref], [Google Scholar], [Publisher]
[95]. Urbankowski P., Anasori B., Hantanasirisakul K., Yang L., Zhang L., Haines B., May S.J., Billinge S.J., Gogotsi Y. *Nanoscale*., 2017, **9**:17722 [Crossref], [Google Scholar], [Publisher]
[96]. Tang H., Yang Y., Wang R., Sun J. *J. Mater. Chem. C*., 2020, **8**:6214 [Crossref], [Google Scholar], [Publisher]
[97]. Iqbal A., Shahzad F., Hantanasirisakul K., Kim M.-K., Kwon J., Hong J., Kim H., Kim D., Gogotsi Y., Koo C. *Sci*., 2020, **369**:446 [Google Scholar], [Publisher]
[98]. Ling Z., Ren C.E., Zhao M.-Q., Yang J., Giammarco J.M., Qiu J., Barsoum M.W., Gogotsi Y. *PNAS*., 214, **111**:16676 [Crossref], [Google Scholar], [Publisher]
[99]. Wang H., Zhang J., Wu Y., Huang H., Li G., Zhang X., Wang Z. *Applied Surface Science*., 2016, **384**:287 [Crossref], [Google Scholar], [Publisher]
[100]. Ma X., Liu Y., Zhang Q., Sun S., Zhou X., Xu Y. *J. Clean. Prod*., 2022, **331**:129878 [Crossref], [Google Scholar], [Publisher]
[101]. Tochetto G., Simão L., de Oliveira D., Hotza D., Immich A. *Clean. Prod*., 2022, 133982 [Crossref], [Google Scholar], [Publisher]
[102]. Velmurugan G., Siva Shankar V., Natrayan L., Sekar S., Patil P.P., Kumar M.S., Thanappan S. *Adsorpt. Sci. Technol*., 2022, **2022**:[Crossref], [Google Scholar], [Publisher]
[103]. Wang L., Peng M., Chen J., Tang X., Li L., Hu T., Yuan K., Chen Y. *ACS nano*., 2022, **16**:2877 [Crossref], [Google Scholar], [Publisher]
[104]. Chen J., Shen Z., Kang Q., Qian X., Li S., Jiang P., Huang X. *Sci. Bull*., 2022, **67**:609 [Crossref], [Google Scholar], [Publisher]
[105]. Nahian M.S., Jayan R., Kaewmaraya T., Hussain T., Islam M.M. *ACS Appl. Mater. Interfaces*., 2022, **14**:10298 [Crossref], [Google Scholar], [Publisher]
[106]. Wang H., Cui Z., He S.-A., Zhu J., Luo W., Liu Q., Zou R. *Nanomicro Lett*., 2022, **14**:189 [Crossref], [Google Scholar], [Publisher]
[107]. Qu H., Deng J., Peng D., Wei T., Zhang H., Peng R. *Processes*., 2022, **10**:641 [Crossref], [Google Scholar], [Publisher]
[108]. Pellenz L., de Oliveira C.R.S., da Silva Júnior A.H., da Silva L.J.S., da Silva L., de Souza A.A.U., Ulson S.M.d.A.G., Borba F.H., da Silva A. *Separation and Purification Technology*, 2023, 305:122435 [Crossref], [Google Scholar], [Publisher]
[109]. Antonelli R., Malpass G.R.P., da Silva M.G.C., Vieira M.G.A.J. *J. Environ. Chem. Eng*., 2020, **8**:104553 [Crossref], [Google Scholar], [Publisher]
[110]. Iqbal A., Hong J., Ko T.Y., Koo C.M. *Nano Converg*., 2021, **8**:1 [Crossref], [Google Scholar], [Publisher]
[111]. Wang W.T., Batool N., Zhang T.H., Liu J., Han X.F., Tian J.H., Yang R.J. *J. Mater. Chem. A*., 2021, **9**:3952 [Crossref], [Google Scholar], [Publisher]
[112]. Gan D., Huang Q., Dou J., Huang H., Chen J., Liu M., Wen Y., Yang Z., Zhang X., Wei Y. *Appl. Surf. Sci*., 2020, **504**:144603 [Crossref], [Google Scholar], [Publisher]
[113]. Shahzad A., Rasool K., Miran W., Nawaz M., Jang J., Mahmoud K.A., Sung Lee D. *ACS*

Sustainable Chem. Eng., 2017, **5**:11481 [Crossref], [Google Scholar], [Publisher]
[114]. Karthikeyan P., Ramkumar K., Pandi K., Fayyaz A., Meenakshi S., Park C.M. *Ceram. Int.,* 2021, **47**:3692 [Crossref], [Google Scholar], [Publisher]
[115]. Halim J., Cook K.M., Eklund P., Rosen J., Barsoum M.W. *Appl. Surf. Sci*., 2019, **494**:1138 [Crossref], [Google Scholar], [Publisher]
[116]. Natu V., Benchakar M., Canaff C., Habrioux A., Celerier S., Barsoum M.W. *Matter*., 2021, **4**:1224 [Crossref], [Google Scholar], [Publisher]
[117]. Jun B.-M., Heo J., Taheri-Qazvini N., Park C.M., Yoon Y. *Ceram. Int*., 2020, **46**:2960 [Crossref], [Google Scholar], [Publisher]
[118]. Wang X., Ong G.M., Naguib M., Wu J. *J. Phys. Chem. C*., 2021, **125**:21771 [Crossref], [Google Scholar], [Publisher]
[119]. Jeon M., Jun B.-M., Kim S., Jang M., Park C.M., Snyder S.A., Yoon Y. *Chemosphere*., 2020, **261**:127781 [Crossref], [Google Scholar], [Publisher]
[120]. Jamaluddin N.S., Alias N.H., Samitsu S., Othman N.H., Jaafar J., Marpani F., Lau W.J., Tan Y. *J. Environ. Chem. Eng*., 2022, **10**:108665 [Crossref], [Google Scholar], [Publisher]
[121]. Lim S., Kim J.H., Park H., Kwak C., Yang J., Kim J., Ryu S.Y., Lee J. *RSC advances*., 2021, **11**:6201 [Crossref], [Google Scholar], [Publisher]
[122]. Bilal M., Ihsanullah I. *JWPE*., 2022, **49**:103010 [Crossref], [Google Scholar], [Publisher]
[123]. Fard A.K., Mckay G., Chamoun R., Rhadfi T., Preud'Homme H., Atieh M. *J. Chem. Eng*., 2017, **317**:331 [Crossref], [Google Scholar], [Publisher]
[124]. Yan J., Liu P.F., Wen H.X., Liu H. *ChemistrySelect*., 2022, **7**:e202201733 [Crossref], [Google Scholar], [Publisher]
[125]. Wang S., Wang L., Li Z., Zhang P., Du K., Yuan L., Ning S., Wei Y., Shi W. *J. Hazard. Mater*., 2021, **408**:124949 [Crossref], [Google Scholar], [Publisher]
[126]. Ilyas M., Younas M., Shah M.U.H., Rehman W.U., Rehman A.U., Yuan Z.-H., Zheng Y.-M., Sheikh M., Rezakazemi M. *JWPE*., 2023, **55**:104131 [Crossref], [Google Scholar], [Publisher]
[127]. Jun B.-M., Jang M., Park C.M., Han J., Yoon Y. *Nucl. Eng. Technol*., 2020, **52**:1201 [Crossref], [Google Scholar], [Publisher]
[128]. Yan Y., Han H., Dai Y., Zhu H., Liu W., Tang X., Gan W., Li H. *ACS Appl. Nano Mater*., 2021, **4**:11763 [Crossref], [Publisher]
[129]. Ihsanullah I. *J. Chem. Eng*., 2020. **388**:124340 [Crossref], [Google Scholar], [Publisher]
[130].Hu X., Chen C., Zhang D., Xue Y. *Chemosphere*., 2021, **278**:130206 [Crossref], [Google Scholar], [Publisher]
[131].Wang X., Xu Q., Zhang L., Pei L., Xue H., Li Z. *J. Environ. Chem. Eng*., 2023, **11**:109206 [Crossref], [Google Scholar], [Publisher]
[132].Liu D., Li T., Sun W., Zhou W., Zhang G. *ACS Omega*., 2022, **7**:31945 [Crossref], [Google Scholar], [Publisher]
[133].Tunesi M.M., Soomro R.A., Han X., Zhu Q., Wei Y., Xu B. *Nano Converg.,* 2021, **8**:5 [Crossref], [Google Scholar], [Publisher]
[134].Wei Z., Peigen Z., Wubian T., Xia Q., Yamei Z., ZhengMing S. *Mater. Chem. Phys.,* 2018, **206**:270 [Crossref], [Google Scholar], [Publisher]
[135].Cai C., Wang R., Liu S., Yan X., Zhang L., Wang M., Tong Q., Jiao T. *Colloids Surf. A Physicochem. Eng. Asp.,* 2020, **589**:124468 [Crossref], [Google Scholar], [Publisher]
[136]. Feng Y., Wang H., Xu J., Du X., Cheng X., Du Z., Wang H. *J. Hazard. Mater.,* 2021, **416**:125777 [Crossref], [Google Scholar], [Publisher]
[137]. Vakili M., Cagnetta G., Huang J., Yu G., Yuan J. *Molecules*., 2019, **24**:2478 [Crossref], [Google Scholar], [Publisher]

[138]. Ghani A.A., Shahzad A., Moztahida M., Tahir K., Jeon H., Kim B., Lee D.S. *J. Chem. Eng*., 2021, **421**:127780 [Crossref], [Google Scholar], [Publisher]
[139]. Ghani A.A., Kim B., Nawaz M., Devarayapalli K.C., Lim Y., Kim G., Lee D.S. *J. Chem. Eng*., 2023, **467**:143473 [Crossref], [Google Scholar], [Publisher]
[140]. Shahzad A., Rasool K., Miran W., Nawaz M., Jang J., Mahmoud K.A., Lee D.S. *ACS Sustain. Chem. Eng*., Engineering. 2017, **5**:11481 [Crossref], [Google Scholar], [Publisher]
[141]. Xu M., Huang C., Lu J., Wu Z., Zhu X., Li H., Xiao L., Luo Z. *Molecules*., 2021, **26**:3150 [Crossref], [Google Scholar], [Publisher]
[142]. Jun B.-M., Park C.M., Heo J., Yoon Y. *J. Environ. Manage*., 2020, **256**:109940 [Crossref], [Google Scholar], [Publisher]
[143]. Dao X., Hao H., Bi J., Sun S., Huang X. *Ind. Eng. Chem. Res*., 2022, **61**:6028 [Crossref], [Google Scholar], [Publisher]
[144]. Zeng X., Wang Y., He X., Liu C., Wang X., Wang X. *J. Environ. Chem. Eng*., 2021, **9**:106203 [Crossref], [Google Scholar], [Publisher]
[145]. Mashtalir O., Cook K.M., Mochalin V.N., Crowe M., Barsoum M.W., Gogotsi Y.J. *J. Mater. Chem. A*., 2014, **2**:14334 [Crossref], [Google Scholar], [Publisher]
[146]. Lin Q., Zeng G., Yan G., Luo J., Cheng X., Zhao Z., Li H.J. *J. Chem. Eng*., 2022, **427**:131668 [Crossref], [Google Scholar], [Publisher]
[147]. Rethinasabapathy M., Bhaskaran G., Park B., Shin J.-Y., Kim W.-S., Ryu J., Huh Y.S. *Chemosphere*., 2022, **286**:131679 [Crossref], [Google Scholar], [Publisher]
[148]. Ahmaruzzaman M. *Inorg. Chem. Commun*., 2022, 109705 [Crossref], [Google Scholar], [Publisher]
[149]. Chaudhuri H., Yun Y.-S.J.S., Technology P. 2022, **297**:121518 [Crossref], [Google Scholar], [Publisher]
[150]. Wu Z., Deng W., Tang S., Ruiz-Hitzky E., Luo J., Wang X. *Chem. Eng J*., 2021, **426**:130776 [Crossref], [Google Scholar], [Publisher]
[151]. Zhang Y., Wang L., Zhang N., Zhou Z. *RSC adv*., 2018, **8**:19895 [Crossref], [Google Scholar], [Publisher]
[152]. Li S., Lu J., Zou D., Cui L., Chen B., Wang F., Qiu J., Yu T., Sun Y., Jing W. *Chem Eng J*., 2023, **457**:141217 [Crossref], [Google Scholar], [Publisher]
[153]. Sun B., Dong X., Li H., Shang Y., Zhang Y., Hu F., Gu S., Wu Y., Gao T., Zhou G. *Sep. Purif. Technol*., 2021, **272**:118964 [Crossref], [Google Scholar], [Publisher]
[154]. Xue H., Gao X., Seliem M.K., Mobarak M., Dong R., Wang X., Fu K., Li Q., Li Z. *J. Chem. Eng*., 2023, **451**:138735 [Crossref], [Google Scholar], [Publisher]
[155]. Yang G., Hu X., Liang J., Huang Q., Dou J., Tian J., Deng F., Liu M., Zhang X., Wei Y. *J Hazard Mater*., 2021, **419**:126220 [Crossref], [Google Scholar], [Publisher]
[156]. Ramanavicius S., Ramanavicius A. *Int. J. Mol. Sci*., 2020, **21**:9224 [Crossref], [Google Scholar], [Publisher]
[157]. Wang Q., Pan X., Wang X., Cao S., Chen L., Ma X., Huang L., Ni Y. *Ceram. Int*., 2021, **47**:4398 [Crossref], [Google Scholar], [Publisher]
[158]. Bhat A., Anwer S., Bhat K.S., Mohideen M.I.H., Liao K., Qurashi A. *NPJ 2D Mater. Appl*., 2021, **5**:61 [Crossref], [Google Scholar], [Publisher]
[159]. Junkaew A., Arroyave R. *Phys. Chem. Chem. Phys*., 2018, **20**:6073 [Crossref], [Google Scholar], [Publisher]
[160]. Vakili M., Cagnetta G., Huang J., Yu G., Yuan J. *Molecules.,* 2019, **24**:2478 [Crossref], [Google Scholar], [Publisher]
[161]. Ghani A.A., Shahzad A., Moztahida M., Tahir K., Jeon H., Kim B., Lee D.S. *J. Chem. Eng.*,2021, **421**:127780 [Crossref], [Google Scholar], [Publisher]

[162]. Sheth Y., Dharaskar S., Chaudhary V., Khalid M., Walvekar R. *Chemosphere*., 2022, 133563 [Crossref], [Google Scholar], [Publisher]
[163]. Karthikeyan P., Elanchezhiyan S.S., Preethi J., Talukdar K., Meenakshi S., Park C.M. *Ceram. Int*., 2021, **47**:732 [Crossref], [Google Scholar], [Publisher]
[164]. Shi X.y., Gao M.h., Hu W.w., Luo D., Hu S.z., Huang T., Zhang N., Wang Y. *Sep. Purif. Technol*., 2022, **287**:120596 [Crossref], [Google Scholar], [Publisher]

How to cite this manuscript: Farhad Ali, Shafaq Zahid, Shakir Khan, Shafi Ur Rehman, Fawad Ahmad. A Comprehensive Review on Adsorption of Dyes from Aqueous Solution by Mxenes. *Asian Journal of Green Chemistry*, 8(1) 2024, 81-107.
DOI: 10.48309/ajgc.2023.412227.1435